Classical density functional theory & simulations on a coarse-grained model of aromatic ionic liquids.

Turesson, Martin; Szparaga, Ryan; Ma, Ke; Woodward, Clifford E; Forsman, Jan

Published in:
Soft Matter

DOI:
10.1039/c3sm53169d

2014

Classical Density Functional Theory & simulations on a coarse-grained model of aromatic ionic liquids

Martin Turesson*, Ryan Szparaga*, Ke Ma**, Clifford E. Woodward** and Jan Forsman*
Theoretical Chemistry, Lund University
P.O.Box 124, S-221 00 Lund, Sweden
*School of Physical, Environmental and Mathematical Sciences
University College, University of New South Wales, ADFA
Canberra ACT 2600, Australia

January 22, 2014

Abstract

A new *classical* density functional approach is developed to accurately treat a coarse-grained model of room temperature aromatic ionic liquids. Our major innovation is the introduction of charge-charge correlations, which are treated in a simple phenomenological way. We test this theory on a generic coarse-grained model for aromatic RTILs with oligomeric forms for both cations and anions, approximating *1-alkyl-3-methyl imidazoliums* and BF_4^-, respectively. We find that predictions by the new density functional theory for fluid structures at charged surfaces are very accurate, as compared with molecular dynamics simulations, across a range of surface charge densities and lengths of the alkyl chain. Predictions of interactions between charged surfaces are also presented.

1 Introduction

Room-temperature ionic liquids (RTILs) are salts which are liquid at temperatures less than 100 °C. This property is imparted to them by the steric effects of oligomeric groups which hinder crystallization. These liquids are electrically conducting albeit with a high viscosity and have negligible vapour pressure. These properties are tunable from the point of view of chemical structure, as the number of different combinations of anions and cations that form RTILs is huge.[1,2] Some RTILs are versatile and powerful solvents, even able to dissolve cellulose.[3] The electrochemical stability and short Debye screening lengths of RTILs also make them an attractive option for use as electrolytes in electric double-layer capacitors (EDLCs), although their dynamic response to electric fields is compromised by their high viscosity. A property of prime importance in EDLCs, is the structure that the constituent electrolyte creates at charged surfaces. For example, RTILs exhibit an adsorption-layer saturation effect at high absolute surface charge density, which causes the differential capacitance to eventually decrease as the absolute surface potential increases. On the other hand, surface depletion of the RTIL at the neutral electrode can cause the differential capacitance to decrease at low potentials as well.[4–7] This can be offset if the neutral electrode surface has a high affinity to the RTIL. These effects combine to generate a (now characteristic) 'camel-shaped' differential capacitance curve.[8] Dilute electrolyte approximations to the Poisson equation (such as the Gouy-Chapman-Stern model) fail to explain this behaviour, so more complex theories have had to be developed.[4,6]

EDLC's generally contain electrodes of exceptional porosity and the rich phase behaviours of RTIL's in nanoscale pores may lead to interesting phenomena. In very narrow pores, the liquid may turn glassy, liquid crystalline, or completely freeze. All-atom simulations by Sha et al.[9] have suggested that a solid phase monolayer exists inside pores of a comparable size to the cation. Surface force measurements by Perkin et al[10] suggest that the nature of the structure at the surface is dependent upon the competition between the electrostatic forces and the excluded volume of the oligomeric units.

Due to their high viscosity, simulations of RTILs display a very slow convergence[11] and, depending upon the phenomenon being studied, using a coarse-grained (CG), rather than all-atom model for the RTIL may be an appealing alternative.[12,13] By removing some degrees of freedom from the system, the Hamiltonian becomes essentially an effective *free energy*, and allows one to model the RTIL more simply. The computational cost can be significantly reduced and hence allow the simulations of larger systems, over a longer time-frame.[14] CG models consist of simple connected spheres, possessing partial charges and dispersion interactions, thus they have the added advantage of reducing the number of (adjustable) model parameters. Hence, these simplified models are better able to highlight the most important physical mechanisms of the system under study, albeit with an associated loss of accuracy. In studies of various fluid phenomena, for example, those involving phase transitions or due to general structural trends, coarse-grained models are invaluable tools to elucidate physical mechanisms. This is also true of ionic liquids.

The simplifications enjoyed by the use of CG models may still not be sufficient to alleviate all the time-consuming aspects of computer simulations. A ubiquitous example are studies which couple bulk and non-uniform environments (such as RTILs in pores or adjacent to electrodes). These simulations are difficult to perform, due to problems in maintaining a constant chemical potential. Usually a large bulk reservoir needs to be included explicitly within the simulations, at significant computational cost. For this reason other theoretical methods, *albeit* approximate ones, are an attractive alternative to simulations. More analytical theoretical methods become viable options when CG models are used, as has been demonstrated in the growing number of such studies reported in the literature.[4,15–19] Analytical theoretical treaments are an important compliment to simulation studies, as they often allow physical insights to be drawn, at a computational cost which often is many orders of magnitude lower than is required for simulations.

A major problem in the theoretical treatment of RTILs, which makes it hard to circumvent the use of simulations, is the high degree of electrostatic and steric coupling. This presents a stringent challenge to any analytical theoretical method used to analyze them. This notwithstanding, several different (non-simulation) theoretical approaches have emerged in recent years. These include lattice-based theories, which emphasize the steric contributions to the free energy (beyond mean-field electrostatics)[4] as well as localized dielectric response.[15,16] Other workers have modelled correlations using an approximate two-particle direct correlation function (from the mean spherical approximation)[17,18] or have used a modified Poisson-Boltzmann treatment.[19] Most (if not all) of these approaches can be considered as different forms of classical density functional theory. In some cases novel behaviours of RTILs have been predicted, e.g., oscillatory differential capacitance.[17] All these treatments use CG models for the RTIL. However, their accuracy has generally not been tested against computer simulations of the *same* coarse-grained model.

Recently, we developed a non-perturbative DFT that implemented electrostatic correlation expressions derived from an extended Debye-Hückel approach to one-component plasmas.[6] In that work we used a simple CG model of the RTIL, which facilitated our semi-analytical approach. While our theory was also successful in producing novel differential capacitance behaviour, comparisons with Monte Carlo simulations of the same CG model highlighted some discrepancies. In this work, we aim to correct the deficiencies of our DFT, by developing more accurate treatment of electrostatic correlations. To do this, we have used a phenomenological approach whereby the correlation contributions remain

mathematically simple, yet are motivated by well-established physical considerations. The ultimate accuracy of the theory is ascertained by Monte Carlo and Molecular Dynamics simulations, within the framework of the CG models.

The CG model we will use in this study is slightly more complex than that used in.[6] In common with that model, it consists of simple bonded beads containing partial charges and interacting via Lennard-Jones forces. While this general model can be optimized to fit a range of RTILs we will focus on a cation structure which roughly matches the homologous series of *1-alkyl-3-methyl imidazoliums* , C_nMIM^+, where n denotes the length of the alkyl chain. The anion will approximate *tetrafluoroborate* ion, BF_4^-. We emphasize that the model parameters chosen in the present study, are not *fully* optimized to the physical properties of these RTILs *per se*. Rather, the purpose of this study is to highlight the performance of our new classical DFT, for a generic set of CG model parameters. That is, the CG model we use here is expected to be representative of a general class of RTILs, but further refinement of its parameters would be needed to make the model optimal for a particular ionic liquid.

2 Model and Theory

2.1 RTIL model

In this section we will describe the features of the CG model used in this study. Our aim is to broadly mimic the homologous series of 1-alkyl-3-methyl imidazolium cations combined with the tetrafluoroborate anion. The model should be simple and contain as few parameters as possible, and easily generalized to describe the homologous series. In addition, the model should be possible to treat accurately via DFT methods. With these criteria in mind, we chose to mimic the molecular architecture of the RTIL with connected neutral and charged spheres. The DFT has been very successfully applied to oligimeric fluids consisting of hard sphere monomers and we propose to take advantage of this in our ionic liquid model. Our proposed model is illustrated in Figure 1. Here the CH_2 and CH_3 groups

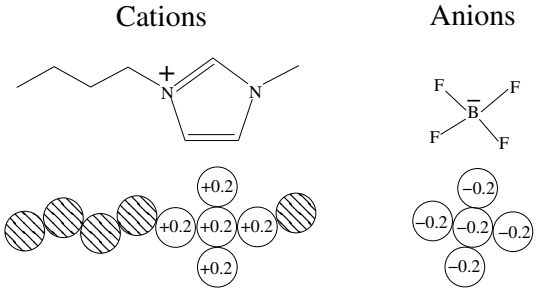

Figure 1: A cartoon of our RTIL model of $[C_4MIM^+][BF_4^-]$. The spheres are tangentially connected and freely jointed.

in the C_nMIM^+ cation are modeled with neutral spheres, using a so-called *united atom* strategy common in CG models. The imidazolium group consists of a star-like structure of tangentially connected, freely jointed spherical beads, each carrying +0.2 elementary charges. The anion has an identical structure to the imidazolium moiety with each sphere carrying a -0.2 charge, again mimicking a disperse charge distribution. The homologous series is built up by sequentially adding neutral CH_2 spheres to the cation model. The nomenclature, $C_nMIM(n = 2, 3, 4, ..)$ will be used to denote the members of the series.

All beads are assumed to interact with each other via a pairwise additive Lennard-Jones interaction:

$$\phi_{LJ}(r) = 4\epsilon_{LJ}\big[(\frac{\sigma}{r})^{12} - (\frac{\sigma}{r})^{6}\big]. \quad (1)$$

Here r is the separation between sphere centers and ϵ_{LJ} and σ determine the attractive strength and the repulsive range of the of the dispersion interaction, respectively. For convenience we will assume that *all* species have the same values for these parameters, i.e., all constituent spheres have the same mutual dispersion interactions. The size parameter σ is also assumed to be the fixed bond distance between connected spherical beads. We should note that this simple parameter choice is for convenience, and in line with our aim for a generic model. Subsequent fine-tuning of these values, e.g., differentiating parameter values for different groups within the molecules, would be required for refined models of *specific* RTILs. Here, we are interested in the ability of our new DFT to treat this generic model, which is only *representing* a class of RTILs, inspired by the structure of the imidazolium series. We set $\sigma = 2.4$ Å, a value that is reasonable for the chemical species that are modeled by the spheres. The strength parameter, ϵ_{LJ}, was then chosen so that the experimentally determined densities of C_nMIM in the bulk liquid are reproduced in our simulations, at ambient pressure and temperature. A surprising result was that this could be essentially achieved with a *single* value of $\epsilon_{LJ} = 100k_BK$, where k_B is Boltzmann's constant. We will present the numerical comparisons with experimental density data below.

All charged species also interact via the Coulomb potential,

$$\phi_{el}^{\alpha\beta}(r) = \frac{z_\alpha z_\beta e^2}{4\pi\epsilon_0\epsilon_r r} \tag{2}$$

where z_α and z_β are the valencies of the interacting pair, e is the elementary charge and ϵ_0 is the permittivity of vacuum. The relative permittivity, ϵ_r (due to the electronic polarizability) is set equal to that of benzene, i.e. $\epsilon_r = 2.3$. The choice of this value was inspired by the aromatic structure of the anion in this class of RTILs.

2.2 Density Functional Theory

In classical density functional theory (DFT), the free energy is expressed as a functional of the particle densities and then minimized with respect to the latter in order to determine the corresponding equilibrium values. The DFT approach can be used to determine bulk properties as well as structural properties in the presence of surfaces, such as capacitance in confined geometries or even surface forces between charged particles.

As the CG model is oligomeric, a *polymer* version of DFT is required.[20] Using a now standard formulation, the Helmholtz free energy is written as a sum of ideal and excess contributions,

$$\mathcal{F}[\{N_\alpha(\mathbf{R})\}] = \mathcal{F}^{id}[\{N_\alpha(\mathbf{R})\}] + \mathcal{F}^{ex}[\{N_\alpha(\mathbf{R})\}]. \tag{3}$$

where $\{N_\alpha(\mathbf{R}); \alpha = a, c\}$ are the set of oligomeric densities describing the anions (a) and cations (c). Here $\mathbf{R}$ represent the positions of the constituent spheres of the ions. The ideal chain term is given by:[20,21]

$$\beta\mathcal{F}^{id} = \sum_{\alpha=a,c}\int N_\alpha(\mathbf{R})\left(\ln[N_\alpha(\mathbf{R})] - 1\right)d\mathbf{R} + \beta\sum_{\alpha=a,c}\int N_\alpha(\mathbf{R})(V_\alpha^{(B)}(\mathbf{R}) + V_\alpha^{ex}(\mathbf{R}))d\mathbf{R}, \tag{4}$$

where $V_\alpha^{(B)}(\mathbf{R})$ is the bonding energy and $V_\alpha^{ex}(\mathbf{R})$ is the external force field.

The mean-field electrostatic contribution to the excess free energy is given by the following expression,

$$\mathcal{F}_{el}^{mf} = \frac{1}{2}\int\int\sum_\alpha\sum_\lambda n_\alpha(\mathbf{r})n_\lambda(\mathbf{r}')\phi_{el}^{\alpha\lambda}(|\mathbf{r}-\mathbf{r}'|)d\mathbf{r}d\mathbf{r}' + \int\sum_\alpha V_{el}(\mathbf{r})n_\alpha(\mathbf{r})d\mathbf{r} + E_{surf} \tag{5}$$

Here $\{n_\alpha(\mathbf{r}); \alpha = a, c\}$ are the charge site densities of anions and cations. These are defined as

$$n_\alpha(\mathbf{r}) = \int d\mathbf{R}\sum_i \delta(\mathbf{r} - \mathbf{r}_i)N_\alpha(\mathbf{R}) \tag{6}$$

where $\delta(\mathbf{r})$ is a Dirac delta function, and the sum is over all the charged sites on species α. The quantity $V_{el}(\mathbf{r})$ represents the potential due to external charges, and E_{surf} denotes the mutual interactions of those external charges.

As is common in DFT theory, we shall assume that all the contributing terms to the excess free energy are functionals only of the monomeric particle densities, such as the charge site densities, $n_c(\mathbf{r})$ and $n_a(\mathbf{r})$, defined above. It is also convenient to define the neutral bead density $n_n(\mathbf{r})$, which is defined analogously to the charge site densities (but one sums over neutral sites on both anions and cations instead). Finally, the total bead density $n_s(\mathbf{r})$ is defined as $n_s(\mathbf{r}) = n_c(\mathbf{r}) + n_a(\mathbf{r}) + n_n(\mathbf{r})$.

A simple, mean-field expression to describe the dispersion interaction between beads is given by,

$$\mathcal{F}_{disp} \approx \frac{1}{2} \int \int_{|\mathbf{r}-\mathbf{r}'|)\geq\sigma} n_s(\mathbf{r}) n_s(\mathbf{r}') \phi_{disp}(|\mathbf{r}-\mathbf{r}'|) d\mathbf{r} \tag{7}$$

where

$$\phi_{disp}(r) = -4\epsilon_{LJ}(\frac{\sigma}{r})^6 \tag{8}$$

If only ideal and mean-field electrostatic and dispersion terms are used in the DFT, then one obtains a generalized polymer Poisson-Boltzmann theory for the ionic liquid. Such an approach completely ignores:

- excluded volume (steric) effects, due to the inability of particles to overlap at short separations
- attractive correlations due to dispersion forces
- charge-charge correlations due to soft repulsions between like charges and attractions between and unlike charges

We will consider these correlation contributions below on a term by term basis.

2.2.1 Excluded volume

Excluded volume correlations have already been treated successfully by us in a polymer DFT applied to hard sphere chains.[20,21] In the current application one needs to define a weighted density over all monomers (as originally suggested by Nordholm *et al.*[22] in the context of a generalized van der Waals theory for simple hard spheres),

$$\bar{n}_s(\mathbf{r}) = \frac{3}{4\pi\sigma^3} \int_{|\mathbf{r}-\mathbf{r}'|<\sigma} n_s(\mathbf{r}') d\mathbf{r}'. \tag{9}$$

This weighted density is then used as input into the excess hard-sphere term from an appropriate polymer equation of state. We chose to use the Generalized Flory-Dimer equation of state,[23] which has already provided accurate non-uniform structures in hard core polymer models.[21] Thus this steric correction is a highly non-linear functional of the total monomer density.

2.2.2 Correlations due to dispersion attractions

In order to assess the importance of correlations due to dispersion forces, we performed bulk NPT (constant pressure) MD simulations on our coarse-grained RTIL model, *but where the charges are switched off*, and compared them with density functional calculations wherein only the mean-field dispersion attractions and the excluded volume correlations were included in the excess free energy. The pressure was chosen to give simulated bulk densities comparable to the corresponding "real" (experimental, fully ionized) RTILs. Though the simulations employed "soft spheres" (a full Lennard-Jones potential was used) while Eq.(8) was used for DFT calculations, we found that the resulting bulk densities from DFT and MD simulations were reasonably similar (see Figure 2), for the various alkyl lengths. In

particular, the agreement between the DFT and simulations with respect to the trend as a function of the cationic length is quite remarkable. There seems to be a constant difference, with the simulated density about 5% higher than DFT for all chain lengths. The slightly higher bulk density in the simulations can be attributed to the ability for molecules to cluster (see Suporting Information), which is not accounted for directly in DFT. It should be noted that use of Eq.(8), which neglects the soft repulsion of the Lennard-Jones potential, may be viewed as a crude way to capture some effects from dispersion correlations.

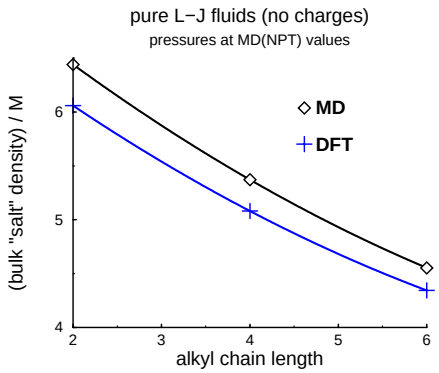

Figure 2: Comparing MD data and DFT predictions for bulk densities of RTIL models of C_nMIM, but where *the charges have been switched off*. The bulk pressures (identical for MD and DFT) were chosen, via MD-NPT, so as to approximately reproduce the corresponding experimental densities (where the RTILs are ionized, of course). This means that the pressures are considerably higher than the atmospheric value.

2.2.3 Electrostatic Correlations

Our general approach with respect to the electrostatic correlation contributions to the excess free energy functional, will be to assume that they are all second-order with respect to the relevant particle densities, i.e.,

$$\mathcal{F}_{corr} \approx \frac{1}{2}\int\int n_\alpha(\mathbf{r})n_\lambda(\mathbf{r}')K^{\alpha\lambda}_{corr}(|\mathbf{r}-\mathbf{r}'|)d\mathbf{r}d\mathbf{r}' \tag{10}$$

The algebraic form of the *correlation kernels*, $K^{\alpha\lambda}_{corr}$, will be physically motivated and will be ultimately chosen to reproduce appropriate thermodynamic properties.

2.2.4 Correlations between like charges

The mean-field expression for the electrostatic interaction, Eq.(5), includes a "self-interaction" term. In dilute electrolytes, this term is expected to be small and delocalized. However, in dense RTILs this self term is localized and contributes a significant repulsive contribution to the mean-field expression, which should be removed. This can be viewed as a "Coulomb hole" in the like-charge density about a given particle. This is a *soft* hole as particles carrying charges of the same sign naturally tend to avoid each other via the long-ranged Coulomb repulsive force.

We shall borrow ideas from an earlier work,[24] and arrive at an approximation for the "Coulomb hole" by first considering the mean-field expression for the bulk Coulomb energy per particle with charge α, e^{mf}_α:

$$e^{mf}_\alpha = 2\pi n^b_\alpha \int_0^\infty \phi^{\alpha\alpha}_{el}(r)dr \tag{11}$$

where n_α^b denotes the (constant) bulk density of α particles. Note that eq.(11) implies a spurious self-interaction. This could be avoided with exclusion sphere, of radius s, centred on the tagged particle (at the origin). Our self-correction objective then leads to the following criterion for s: $n_\alpha^b 4\pi s^3/3 = 1$, i.e.

$$s = \left[\frac{3}{4\pi n_\alpha^b}\right]^{1/3} \tag{12}$$

The corresponding "corrected" energy per particle, e_α^c becomes:

$$\beta e_\alpha^c = 2\pi\beta \int_0^\infty \phi_{el}^{\alpha\alpha}(r)dr - \pi l_B z_\alpha^2 s^2 \tag{13}$$

where β is the inverse thermal energy and $l_B = \frac{\beta e^2}{4\pi\epsilon_0\epsilon_r}$ is the Bjerrum length. The self correction, formulated in this manner, enters in a drastic step-like manner. However, "Coulomb holes" are usually rather soft, we will instead assume that the radial distribution function, $g_{\alpha\alpha}(r)$, displays an exponential approach to unity:

$$n_\alpha^b \to n_\alpha^b(1 - e^{-\lambda_\alpha(r)}) \tag{14}$$

where $r = |\mathbf{r}|$. We choose λ_α such that the corrected energy per particle becomes identical to the one we established with a step-function like g(r), eq. (13). In other words, we require that:

$$\lambda_\alpha = \frac{\sqrt{2}}{s} \tag{15}$$

where s is given in eq.(12).

In principle, a more accurate correction might be obtained if we allow λ_α to be position-dependent. However, the present formulation has the advantage of simplicity. Furthermore, one should note, that in such dense fluids as RTILs charge density variations are usually not as great as those of dilute electrolytes.

2.2.5 Correlations between opposite charges

Interestingly, the attraction between opposite charges can be overestimated by the mean-field expression, Eq.(5). This is due to the fact that the mean-field theory allows complete penetration by opposite charge densities, which in reality is excluded by the steric repulsion between charges. A simple and pragmatic way to effectively correct the mean-field theory is to build in an effective hard sphere exclusion correlation. Thus, the *unlike* Coulombic interactions (between anions and cations) is then given by

$$\mathcal{F}_{el}^{unlike} = \frac{1}{2}\int\int \sum_{\alpha\neq\beta} n_\alpha(\mathbf{r})n_\beta(\mathbf{r}')\Theta(|\mathbf{r}-\mathbf{r}'| - d_{\alpha\beta})\phi_{el}^{\alpha\beta}(|\mathbf{r}-\mathbf{r}'|)d\mathbf{r}d\mathbf{r}' \tag{16}$$

where the Heaviside function is defined as: $\Theta(x) = 1$ for $x > 0$ and $\Theta(x) = 0$ for $x \leq 0$. The parameter $d_{\alpha\beta}$ is a "distance of closest approach" between unlike charged species. As such it should be numerically equal to the sum of the radii of the species, $\sigma_{\alpha\beta}$. However, additional correlations (beyond hard sphere exclusion) between oppositely charged species can be mimicked to some extent by setting $d_{\alpha\beta} = \chi\sigma_{\alpha\beta}$, with χ an adjustable parameter. Given this ansatz, the question then arises as to how χ should be chosen. Recall that ϵ_{LJ} was chosen, so as to obtain agreement between experimental and *simulated* bulk RTIL densities at atmospheric pressure. Hence an obvious choice is to choose χ so that the correct bulk density is obtained in the DFT as well. For C_nMIM this procedure gives rise to the values $\chi = 0.64, 0.71$ and 0.80 for $n = 2, 4, 6$ respectively. The fact that χ is generally less than unity reflects the positive adsorption between unlike ions, which is modelled as a smaller distance of closest approach in our approximate theory.

2.3 Surfaces

To test the model and the DFT, we shall investigate structures and surface interactions in systems where two charged surfaces are separated by an RTIL film. There is complete equilibrium between the confined space and a bulk liquid, i.e. the chemical potential is maintained if the surface separation or surface charge is changed. We will model the surfaces as flat and uniformly charged, extending infinitely in the x and y directions, perpendicular to the z axis (along the surface normal). We let a_s denote the inverse surface charge density. All spherical beads of our RTIL model, irrespective of their charge, also experience a non-electrostatic interaction with the electrodes, obtained by integrating the Lennard-Jones potential over the half-spaces constituting the surfaces,

$$\beta w_{LJ}(z) = 2\pi\epsilon_{LJ}\left[\frac{2}{45}(\frac{\sigma}{z})^9 - \frac{1}{3}(\frac{\sigma}{z})^3\right], \tag{17}$$

where z is the distance from the plane of charge. The total non-electrostatic interaction due to the surfaces, V_{LJ}, is given by the sum of the two separate contributions, i.e., $V_{LJ} = w_{LJ}(z) + w_{LJ}(h-z)$, where h is the distance between the surfaces.

3 Results

3.1 Bulk densities

Before we evaluate the system behavior in non-uniform conditions, we will demonstrate that our simple coarse-grained model produces a reasonable scaling of the bulk density with respect to the length of the oligomeric chains of the cation species. Initially, the Lennard-Jones strength parameter, ϵ_{LJ} was fitted so that our NPT simulations reproduced the experimental bulk density of C_4MIM (given all other model parameters were fixed at their values described in the previous section). This gave $\epsilon_{LJ} = 100k_bK$. This value was then assumed the same for all C_nMIM models, irrespective of the length (n) of the alkyl chain. In Figure 3, we see that this generates simulated bulk densities which are in very good agreement with experiments for the investigated range of chain lengths, i.e., $n = 2, 4, 6$. This result lends support to the notion that our coarse-grained model captures the essential physics of this class of RTILS.

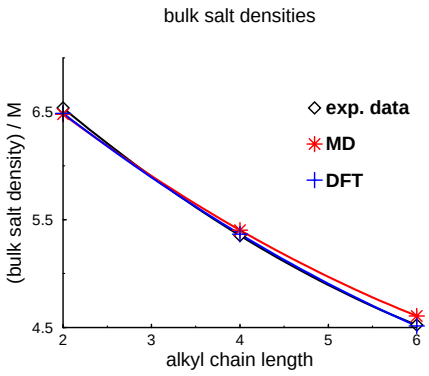

Figure 3: Bulk salt densities of C_nMIM, for various lengths n of the alkyl chain. Experimental data are compared with MD simulation and DFT values, at 294 K and ambient pressure.

3.2 Structural comparisons

In this section we focus on evaluating the (in-house) DFT, by comparing with results obtained from Molecular Dynamics (MD) simulations (GROMACS version 4.5.4 [25]). In these simulations it is convenient to solve the dynamics using harmonic potentials between bonded spheres and where the confining surfaces are built up with discrete charges, rather than a uniform surface charge density. For more details, see the Supporting Information. On the other hand, a different simulation approach using the Metropolis Monte Carlo (MC) algorithm, has the advantage that it is relatively straightforward to treat the same model system as is assumed in the DFT approach. The main drawback is that the MC simulations run considerably more slowly than MD for such dense systems, at least on our multiprocessor machines.

3.2.1 MC vs. MD simulation results

In Figure 4, density profiles obtained with (in-house) MC simulations, for our model of C_2MIM are compared with corresponding data from MD simulations. The agreement is nearly perfect. Hence, in our simulation studies reported below, we have used the much faster MD approach, confident that the slight model differences will only produce minor changes in system properties.

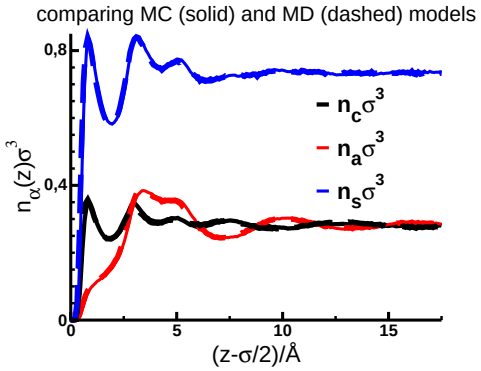

Figure 4: Comparing density profiles as obtained via MD and MC simulations of our model of C_2MIM. In the former case, however, there are (for practical reasons) slight deviations from the model. Specifically, the surface charge is in MD generated by discrete charges, of low valency, and bonds within cat- and anions are (in MD) modelled by an harmonic potential. Details and further tests are provided in the Supporting Information.

3.2.2 DFT evaluations

In Figure 9, we compare DFT predictions with simulation data focusing on the structure of C_4MIM in the vicinity of surfaces with varying surface charge densities. While there are inevitable deviations, the DFT performs remarkably well, seemingly capturing all the important physical characteristics of the profiles. The largest discrepancy is found for the anion density profiles, at negative surfaces, where DFT predicts too strong oscillations, at about 8-12 Å from the surface. Hence one might be tempted to attribute this effect to a failure in the ability of the DFT to account for steric packing effects. However, we have tested replacing our simple weight function (Eq.(9)), by a more elaborate expression suggested by Tarazona [26] for simple hard-spheres. The resulting structural changes following this replacement are barely discernible (not shown), suggesting that other mechanisms (primarily electrostatic) determine the packing of beads in the dense RTIL.

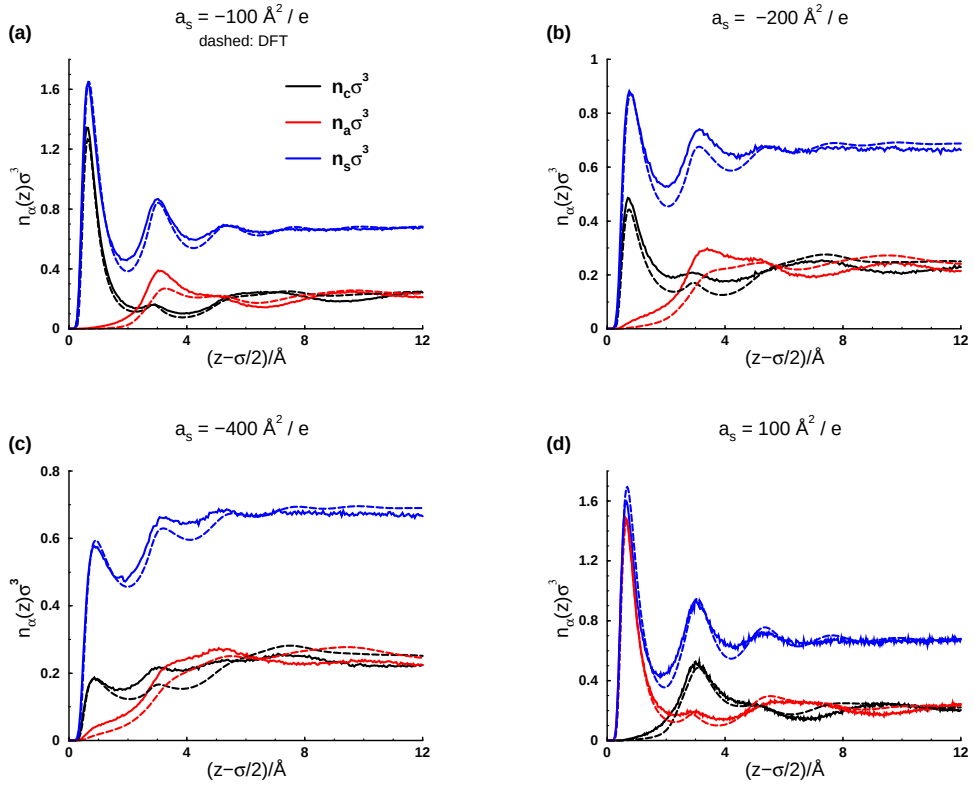

Figure 5: Comparing simulated and calculated (by DFT - dashed lines) density distributions, of C_4MIM adjacent to negatively charged surfaces (at $z = 0$).
(a) $a_s = -100\text{Å}^2/e$
(b) $a_s = -200\text{Å}^2/e$
(c) $a_s = -400\text{Å}^2/e$
(d) $a_s = 100\text{Å}^2/e$

It is instructive to illustrate the importance of correlations, in these highly coupled systems. We will do this via comparisons with predictions from a DFT in which some of these correlations have been removed. Specifically, we removed the "second-order" correlation terms from the DFT, of the type described by Eq.(10), while retaining the higher-order excluded volume correlations. More specifically, the electrostatic correlations were removed by evaluating the Coulomb interactions using the mean-field expression, Eq.(5). Furthermore, we also removed the *subtle* correlations we artificially introduced in our estimate of the dispersion energy. Thus we used the full Lennard-Jones interaction, $\phi_{LJ}(r)$, given by Eq.(1), in place of $\phi_{disp}(r)$ in the dispersion energy term, Eq.(7). In Figure 6, we compare predictions from this reduced correlation form of DFT with the case when all correlations are included. We see that the leaving out these second-order correlations leads to extremely inaccurate predictions, with vastly overestimated density oscillations near the surface. This illustrates the importance of including these correlations within any theoretical treatment of RTILs.

In Figure 7, we have investigated structural properties of our model for C_nMIM ($n = 2, 4, 6$) at a fixed surface charge density. The latter was chosen as a rough estimate of mica, immersed in a typical RTIL. Unfortunately, even an approximate estimate for the surface

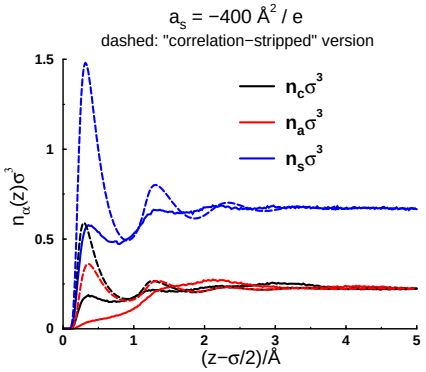

Figure 6: Comparing the performance of our standard model (solid lines), with that obtained by setting $\lambda = 1$, as well as treating Coulomb interactions in a Poisson-Boltzmann (mean-field) manner ("correlation-stripped" version, dashed lines).

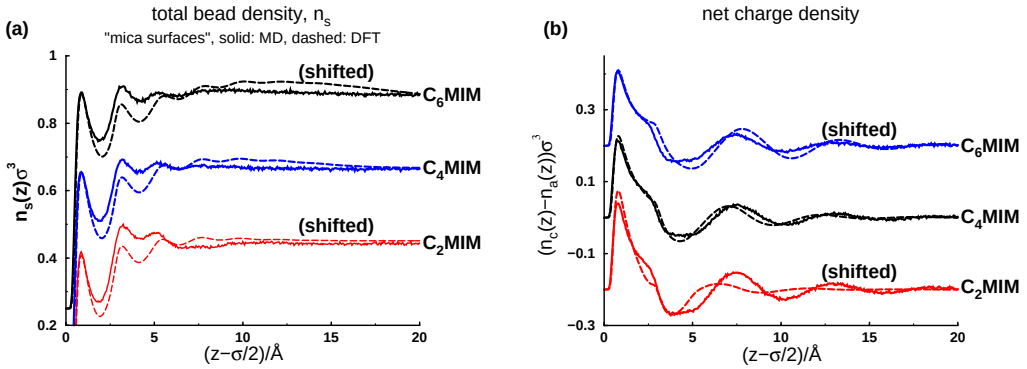

Figure 7: Simulations and DFT predictions of density distributions, for our coarse-grained models of $C_2MIM - C_6MIM$. The inverse charge density is $a_s = -320\text{Å}^2/e$, corresponding to a crude model of mica (see text).

charge density is not straightforward. If we assume that mica is fully charged in water, with a_s = -48 Å$^2/e$ and $\epsilon_r = 80$, a simple Born energy argument suggests that for a typical RTIL dielectric response of $\epsilon_r \approx 12$,[27,28] one would obtain $a_s \approx 48\sqrt{80/12}$ Å$^2/e \approx$ -124 Å$^2/e$. This value deviates considerably from literature estimates, obtained by fitting the double-layer interaction between mica surfaces to a linearized Poisson-Boltzmann expression.[29] In that case, the values obtained ranged between $a_s \approx -670\text{Å}^2/e$ to $a_s \approx -1670\text{Å}^2/e$. In our study here we have used an intermediate value of $a_s = -320\text{Å}^2/e$. At this surface charge density, we find that the DFT is able to accurately predict structure for all three investigated RTILs. This is important, as it allows us to use DFT for predictions of quantities and behaviours that are difficult to obtain with simulations. These include surface forces, differential capacitances, surface tensions and phase equilibria. An interesting observation from Figure 7 is that the interfacial structure is remarkably insensitive to the length of the alkyl chain. The oscillation period for charged beads does seem to increase with chain length, but the effect is very small. This observation is even more unexpected in light of the substantial response of surface interactions to changes of the alkyl chain length, as shown

below.

3.3 Surface forces

In this section, we will investigate surface interactions between negatively charged surfaces, immersed in our models of $C_2MIM - C_6MIM$. We have used an inverse surface charge density of a_s = -320 Å$^2/e$ as a reference, but since this poorly established for a mica surface in an ionic liquid, we will also consider effects from changing this quantity (most experimental surface force measurements are performed with mica surfaces). The results are

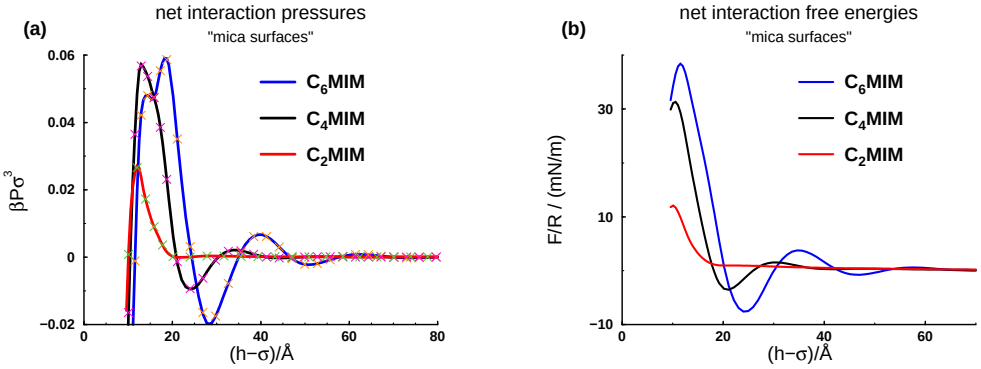

Figure 8: Surface interactions, between uniformly charged surfaces ($a_s \approx -320$Å$^2/e$) in solutions of (our models of) $C_2MIM - C_6MIM$.
(a) Osmotic pressures, as obtained from integrating the force normal to the surfaces (lines) as well as from the negative slope of the free energy vs separation (symbols). The latter symbols are plotted sparsely, for clarity).
(b) Interaction free energies, shown in the experimentally more common form, as force/radius, which implicitly assumes the validity of Derjaguin's Approximation.[30]

presented in Figure 8, which displays osmotic pressures and interaction free energies. The osmotic pressure was evaluated from integrated surface interactions, from first principles. This direct evaluation agrees also with the numerical derivative of the free energy/unit area vs. separation, i.e. the contact value theorem is fulfilled, which is an important thermodynamic consistency check. Figure 8b gives the free energies per unit area, transformed to force/radius via the Derjaguin Approximation.[30] The latter quantity is commonly reported from experimental measurements. A remarkable observation is that the surface interactions are rather sensitive to the alkyl length, despite a modest structural difference. Specifically, we see how the range and strength of the oscillatory forces grow with chain length, which is in qualitative agreement with surface force measurements by Perkin *et al.*, who found similar differences between C_4MIM and C_6MIM, although the anion was different from the BF_4^- used in our model. Furthermore, the force oscillations that they measured, extended to larger separations than we find here, especially for C_6MIM. On the other hand, Min *et al.* only observed minor force oscillations with mica in C_4MIM (with BF_4^- as anion). These, barely detectable, oscillations (as manifested by separation jumps) were superimposed on a monotonic repulsion. The reasons for the discrepancy between these experimental results are not clear to us.

At any rate, it is clear from Figure 8 that the period of oscillation is *not* directly reflected by corresponding density oscillation periods, found at a single surface (cf. Figure 7). Note that similar oscillations also have been found in other experiments on surface interactions in RTILs.[31,32]

Given that the surface charge density is not well established, for mica immersed in ionic liquids, it is of interest to establish how sensitive our predicted surface interactions are to variations of this quantity. Such analyses are provided in Figure 9. An unexpected

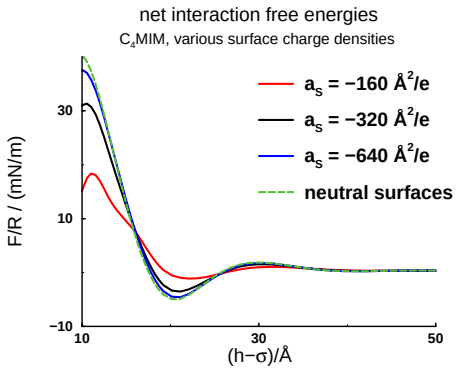

Figure 9: Interactions betwen planar surfaces immersed in $C_2MIM - C_6MIM$. Several different values of uniform inverse surface charge density (a_s) are considered. Interaction free energies are, as in Figure 8, displayed as force/radius, as established via the Derjaguin Approximation.[30]

finding (to us) is that the amplitude of the oscillations *decreases* upon an increase of the surface charge density. We interpret this as a consequence of the RTIL molecules being less free to align in an "amphiphilic" manner, with neutral parts facing the surfaces, when the latter are charged. In other words, such an amphiphilic ordering is partly broken when the surface charge density increases, and this will in turn lead to a drop of the force oscillation amplitudes .

4 Conclusions and outlook

We have proposed a coarse-graining approach for aromatic RTILs. These models can also be treated with accurate classical DFT methods, and the corresponding calculations are quite fast in system geometries that admits at least one dimension to be integrated out. Using experimental bulk densities as a guide, a common value of $\epsilon_{LJ} = 100k_BK$, for bead-bead LJ interactions, was found appropriate for C_4MIM. Using this fixed value for other RTILS, C_2MIM and C_6MIM, our simulation results gave bulk densities also in agreement with experiments. This suggests that our approach for coarse-graining is physically sound. We have developed a new, correlated DFT. This theory uses a single adjustable parameter, namely the effective hard core distance, $d_{\alpha\beta}$, between ions of unlike charge. The correlation-corrected DFT is able to reproduce structural properties obtained from simulations with a remarkable accuracy. Our work is concluded by a DFT study of interactions between charged surfaces confining our coarse-grained models of $C_2MIM - C_6MIM$. Such force curves would be computationally very demanding to produce via simulations. Another advantage of developing a useful and accurate DFT for these systems, is that one is forced to make approximations that identifies and retains the important physics of the system.

Our combination of a simple coarse-grained model, and a correlation-corrected classical DFT forms a very powerful tool for theoretical investigations of RTILs. Areas where simulation approaches are problematic includes differential capacitance in narrow pores, phase transitions and phase equilibria in pores and at electrode surfaces, and interactions between aggregates and surfaces.

References

[1] R. Rogers and K. Seddon, *Ionic Liquids, Industrial Applications to Green Chemistry, ACS Symp. Series 818*, Am. Chem. Soc., Washington, 2002.

[2] S. A. Forsyth, J. M. Pringle and D. R. MacFarlane, *Aust. J. Chem.*, 2004, **57**, 113–119.

[3] R. P. Swatloski, S. K. Spear, J. D. Holbrey and R. D. Rogers, *J. Am. Chem. Soc.*, 2002, **124**, 4974–4975.

[4] A. A. Kornyshev, *J. Phys. Chem. B*, 2007, **111**, 5545–5557.

[5] M. Trulsson, J. Algotsson, J. Forsman and C. E. Woodward, *J. Phys. Chem. Lett.*, 2010, **1**, 1191.

[6] J. Forsman, C. E. Woodward and M. Trulsson, *J. Phys. Chem. B*, 2011, **115**, 4606–4612.

[7] J. Forsman, R. Szparaga, S. Nordholm, C. E. Woodward and R. Penfold, in *Ionic Liquids - Classes and Properties*, InTech, Rijeka, 2011, pp. 127–150.

[8] V. Lockett, R. Sedev, J. Ralston, M. Horne and T. Rodopoulos, *J. Phys. Chem. C*, 2008, **112**, 7486.

[9] M. Sha, G. Wu, Y. Liu, Z. Tang and H. Fang, *J. Phys. Chem. C*, 2009, **113**, 4618–4622.

[10] S. Perkin, L. Crowhurst, H. Niedermeyer, T. Welton, A. M. Smith and N. N. Gosvami, *Chem. Commun.*, 2011, **47**, 6572–6574.

[11] Z. Hu and C. J. Margulis, *Acc. Chem. Res.*, 2007, **40**, 1097–1105.

[12] F. Dommert, J. Schmidt, C. Krekeler, Y. Y. Zhao, R. Berger, L. D. Site and C. Holm, *Journal of Molecular Liquids*, 2010, **152**, 2 – 8.

[13] Y.-L. Wang, A. Lyubartsev, Z.-Y. Lu and A. Laaksonen, *Phys. Chem. Chem. Phys.*, 2013, **15**, 7701–7712.

[14] Y. Wang and G. A. Voth, *J. Am. Chem. Soc.*, 2005, **127**, 12192–12193.

[15] Y. Lauw, M. D. Horne, T. Rodopoulos and F. A. M. Leermakers, *J. Phys. Chem. B*, 2009, **111**, 5545.

[16] Y. Lauw, M. D. Horne, T. Rodopoulos, A. Nelson and F. A. M. Leermakers, *J. Phys. Chem. B*, 2010, **114**, 11149.

[17] D. E. Jiang, D. Meng and J. Z. Wu, *Chem. Phys. Lett.*, 2011, **504**, 153.

[18] J. Z. Wu, T. Jiang, D. E. Jiang, Z. Jin and D. Henderson, *Soft Matter.*, 2011, **7**, 11222.

[19] S. Lamperski, C. Outhwaite and L. Bhuiyan, *J. Phys. Chem.*, 2009, **113**, 8925.

[20] C. E. Woodward, *J. Chem. Phys.*, 1991, **94**, 3183.

[21] J. Forsman and C. E. Woodward, *Macromol.*, 2006, **39**, 1261.

[22] S. Nordholm, M. Johnson and B. C. Freasier, *Aust. J. Chem.*, 1980, **33**, 2139.

[23] K. G. Honnell and C. K. Hall, *J. Chem. Phys.*, 1991, **95**, 4481.

[24] J. Forsman and S. Nordholm, *Langmuir*, 2012, **28**, 4069.

[25] D. van der Spoel, E. Lindahl, B. Hess, E. van Buuren, E. Apol, P. J. Meulenhoff, D. P. Tieleman, A. L. T. M. Sijbers, K. A. Feenstra, R. van Drunen and H. J. C. Berendsen, *Gromacs User Manual version 4.5.4, www.gromacs.org (2010)*.

[26] P. Tarazona and R. Evans, *Molec. Phys.*, 1984, **52**, 847.

[27] J. Sangoro, C. Iacob, A. Serghei, S. Naumov, P. Galvosas, J. Karger, C. Wespe, F. Bordusa, A. Stoppa, J. Hunger, R. Buchner and F. Kremer, *The Journal of Chemical Physics*, 2008, **128**, 214509.

[28] A. Stoppa, J. Hunger, R. Buchner, G. Hefter, A. Thoman and H. Helm, *The Journal of Physical Chemistry B*, 2008, **112**, 4854–4858.

[29] Y. Min, M. Akbulut, J. R. Sangoro, F. Kremer, R. K. Prudhomme and J. Israelachvili, *The Journal of Physical Chemistry C*, 2009, **113**, 16445–16449.

[30] B. V. Derjaguin, *Kolloid Zeits.*, 1934, **69**, 155.

[31] R. Atkin, S. Z. E. Abedin, R. Hayes, L. H. S. Gasparotto, N. Borisenko and F. Endres, *The Journal of Physical Chemistry C*, 2009, **113**, 13266–13272.

[32] R. Hayes, N. Borisenko, M. K. Tam, P. C. Howlett, F. Endres and R. Atkin, *The Journal of Physical Chemistry C*, 2011, **115**, 6855–6863.